J. Appl. Physiol.
88: 373–385, 2000.

Effects of primary resuscitation from shock on distribution of myocardial blood flow

MARTIN KLEEN,[1,2] OLIVER HABLER,[1,2] FRANZ MEISNER,[1]
GREGOR KEMMING,[1,2] ANDREAS PAPE,[1] AND KONRAD MESSMER[1]
[1]*Institute for Surgical Research and* [2]*Department of Anesthesiology, University of Munich, 81366 Munich, Germany*

Kleen, Martin, Oliver Habler, Franz Meisner, Gregor Kemming, Andreas Pape, and Konrad Messmer. Effects of primary resuscitation from shock on distribution of myocardial blood flow. *J. Appl. Physiol.* 88: 373–385, 2000.—Hemorrhagic shock alters heterogeneity of regional myocardial perfusion (RMP) in the presence of critical coronary stenosis in pigs. Conventional resuscitation has failed to reverse these effects. We hypothesized that improvement of the resuscitation regime would lead to restoration of RMP heterogeneity. Diaspirin-cross-linked hemoglobin (10 g/dl; DCLHb) and human serum albumin (8.0 g/dl; HSA) were used. After baseline, a branch of the left coronary artery was stenosed; thereafter, hemorrhagic shock was induced. Resuscitation was performed with either DCLHb or HSA. At baseline, the fractcal dimension (*D*) of subendocardial myocardium was 1.31 ± 0.083 (HSA) and 1.35 ± 0.106 (DCLHb) (mean ± SD). Coronary stenosis increased subendocardial *D* slightly but consistently only in the DCLHb group (1.39 ± 0.104; $P < 0.05$). Shock reduced subendocardial *D*: 1.21 ± 0.093 (HSA; $P = 0.10$), 1.25 ± 0.092 (DCLHb; $P < 0.05$). Administration of DCLHb increased subendocardial *D* in 7 of 10 animals (1.31 ± 0.097; $P = 0.066$). HSA was ineffective in this respect. DCLHb infusion restored arterial pressure and increased cardiac index (CI) to 80% of baseline values. Administration of HSA left animals hypotensive (69 mmHg) and increased CI to 122% of the average baseline value. Shock-induced disturbances of the distribution of RMP were improved by administration of DCLHb but not by HSA.

fractals; spatial heterogeneity; regional perfusion; coronary stenosis; hemoglobin-based oxygen carriers; albumin; pigs

DISTRIBUTION OF REGIONAL myocardial blood flow is strongly heterogeneous (1, 32). This is not merely a result of chance but has been shown to represent the adaptation to regionally different substrate needs (7). Relative dispersion (RD; SD/mean) is a conventionally used measure of spatial perfusion heterogeneity. However, this parameter is dependent on the spatial resolution of the measurement; i.e., RD increases, obeying a power law if spatial resolution of the measurement is increased (1, 32). Comparison of data obtained with different techniques at different scales is therefore inadequate. Clinical perfusion measurements have a much lower resolution than many experimental methods, and technical advances will allow an increase in spatial discrimination of perfusion. These differences in resolution complicate comparison of data from different studies and extrapolation of experimental results to human physiology.

The dilemma has been resolved by the introduction of fractal analysis of myocardial blood flow heterogeneity (1, 32). Fractal analysis relates the increasing resolution of a measurement with the concomitant increase in RD. This relationship obeys a power law. A single parameter, the fractal dimension (*D*), can therefore be determined to describe this relationship. *D* is calculated as 1 minus the slope of the linear relationship between the natural logarithms of measurement resolution and perfusion heterogeneity measured by RD.

The formal relationship is given in *Eq. 1*

$$\log\left(\frac{RD_{(m)}}{RD_{(m_0)}}\right) = (1 - D) \cdot \log\left(\frac{m}{m_0}\right) \qquad (1)$$

The natural logarithm of the relationship of RD measured at some resolution (i.e., mass of myocardial samples; RD_m) and RD measured with the original sample mass [$RD_{(m_0)}$] equals the natural logarithm of the relationship of the respective masses m and m_0 times $1 - D$. If $1 - D$ is the slope of the relationship, $D = 1 -$ slope and can empirically be found from a linear equation obtained by linear regression analysis.

Fractal properties of the coronary vascular tree have been demonstrated (19, 31), and it is not surprising that the RD of regional myocardial perfusion (RMP) is also fractal. Therefore, heterogeneity of RMP lends itself to fractal analysis. Fractal analysis is increasingly accepted to further elucidate the physiology of myocardial blood flow in experimental animals (6, 18, 26, 27). Absolute regional myocardial blood flow can be measured in humans, and heterogeneity of RMP is recognized to be of relevance in coronary artery disease (5, 9). Visser et al. (33) have calculated the *D* of RMP of syndrome X patients and compared these data with data from healthy volunteers. They have shown that *D* is reduced in syndrome X patients.

The *D* of RMP heterogeneity, as calculated from an increasing RD, may vary from 1.0 to 1.5 (1). A *D* value of 1.0 denotes uniform distribution or RMP balanced on all scales of measurement, whereas a *D* value of 1.5 shows that perfusion heterogeneity increases greatly

The costs of publication of this article were defrayed in part by the payment of page charges. The article must therefore be hereby marked "*advertisement*" in accordance with 18 U.S.C. Section 1734 solely to indicate this fact.

with increased resolution and that spatially neighboring myocardial regions display uncorrelated rates of perfusion. A reduction of *D* can also be interpreted as a homogenization of RMP.

Ischemic heart disease is a common condition in surgical patients (23, 23). Therefore, the combination of both coronary stenosis and hypotension or shock is likely to be common in accidental or surgical trauma. The model described in the present report attempts to model this situation in a standardized way. In a previous study we have investigated the effects of this deleterious combination on fractal heterogeneity of RMP for the first time (22). We have shown that hemorrhagic shock decreases the *D* of RMP. Surprisingly, it was found that this effect was not reversed on restoration of hemodynamic determinants of coronary perfusion by means of small-volume resuscitation or conventional fluid therapy (22).

Infusion of diaspirin-cross-linked hemoglobin (DCLHb) has been demonstrated to attenuate postischemic reperfusion injury in hamster muscular tissue (28). Mortality from hemorrhagic shock in rats was reduced to zero by resuscitation with a hemoglobin-based oxygen carrier (HBOC), whereas conventional fluid therapy did not achieve similar results (4). Fluid infusion for treatment of hypovolemia dilutes endogenous hemoglobin and therefore reduces the oxygen transport capacity of blood. Although extreme hemodilution with a HBOC preserves muscle tissue oxygenation, hemodilution to the same degree with conventional colloids is associated with tissue hypoxia (30). Furthermore, a HBOC can increase oxygen delivery to poststenotic tissues beyond the amount supplied by blood without a HBOC (16).

We therefore hypothesized that resuscitation from hemorrhagic shock with DCLHb would be more effective than small-volume resuscitation to reverse shock-induced alterations of the distribution of RMP.

METHODS

This paper represents a further analysis of data from our study published by Habler et al. (13). The aforementioned study does not contain data on the heterogeneity of RMP. To avoid repetition, macrohemodynamic parameters are only briefly summarized.

Animal preparation. We used an animal preparation and technical procedures that have been described before in detail (22, 34). Animals were housed and treated in conformance with German animal-protection legislation. Twenty experiments were performed in open-chest pigs weighing 26 ± 4.2 (SD) kg. The animals were intravenously anesthetized with an opioid [48 μg·kg body wt $(BW)^{-1}\cdot h^{-1}$ fentanyl] and a benzodiazepine (1.2 mg midazolam·kg $BW^{-1}\cdot h^{-1}$), paralyzed with 4 mg/h pancuronium, and mechanically ventilated with 50% oxygen in air. The catheters listed below were inserted into femoral vessels, carotid arteries, or external jugular veins, respectively, after surgical exposure. Animals were instrumented with two micromanometers (PC 370 Millar Instruments, Houston, TX) to measure left ventricular (LV) and aortic pressure. Cardiac output and left anterior descending coronary artery (LAD) flow were assessed with ultrasonic flow probes (diameter 14 and 2 mm; Transonic, Ithaca, NY). For injection of microspheres, a catheter (5F, Arrow, Reading, PA) was inserted into the left atrium through a small incision and secured in place with a circular suture. A critical coronary stenosis was induced by micromanipulator-assisted narrowing of the LAD with a thin, Teflon-coated copper-wire sling distal to the coronary flow probe. Absence of hyperemic response after complete occlusion with a second, more distal, copper wire for 10 s was controlled for to verify the critical degree of stenosis (10).

Microsphere methodology. RMP was measured with radioactive microspheres. The reference-sample technique was used, which allows quantitative determinations (15). For each measurement, one nuclide was randomly selected (^{85}Sr, ^{114}In, ^{95}Nb, ^{141}Ce, ^{46}Sc; diameter 15 ± 0.1 μm; NEN-TRAC, DuPont, Wilmington, DE). The number of microspheres labeled with an individual nuclide in sequential measurements was optimized to reduce methodological error by using specialized software and amounted to $\approx 4.8 \times 10^6 \pm 0.7 \times 10^6$ microspheres/measurement (20). Microspheres were injected slowly into the left atrium while the reference sample was drawn for 3 min from the abdominal aorta through a pigtail catheter (7F, Cordis, Miami, FL) with a calibrated pump at 3.24 ml/min (model 640A, Harvard Apparatus, South Natick, MA). After completion of the protocol, the animals were killed by left atrial injection of potassium chloride. The hearts were removed and fixed in 10% formaldehyde for 4–5 days. Other organs were removed but not analyzed for perfusion heterogeneity. The isolated LV myocardium was dissected into six slices parallel to the base of the heart. Four slices were cut into 12 radial sectors; the most apical slices were dissected into only 10 sectors, which were separated into subendocardial, midmyocardial, and subepicardial samples. In total, 204 LV tissue samples were obtained from each animal, with a mean weight of 331 ± 280 mg. Tissue and reference sample radioactivity were counted for 180 s with a calibrated 1,024-channel gamma counter (model 5650; Packard Instruments, Downers Grove, IL) with a 3-in. NaI (Tl) crystal detector connected to a multichannel analyzer (series 35plus MCA, Canberrra Industries, Meriden, CT). Gamma spectra were separated, background activity was subtracted, and spillover and nuclide decay were corrected with a computer program (MIC-III) (11). RMP was calculated as

$$\dot{Q}_M = I_M \times \frac{\dot{Q}_a}{I_a} \qquad (2)$$

where $\dot{Q}_M$ is regional myocardial blood flow (ml/min), I_M is the intensity of emitted radioactivity from the myocardial tissue sample, $\dot{Q}_a$ is the reference-sample flow (3.24 ml/min), and I_a is the intensity of emitted radioactivity from the reference sample.

Experimental protocol. Baseline values were recorded and microspheres were injected after mean arterial pressure (MAP), heart rate, and cardiac output had been stable for ≈15 min. Results from this measurement are labeled as "baseline" in this report.

A three- to fourfold increase in LAD flow after complete occlusion of the vessel for 10 s was expected as a normal hyperemic response, and this was observed in all animals. After this test, stenosis of the LAD was induced by incremental tightening of the wire sling. Critical stenosis was assumed when hyperemia was absent after 10 s of complete occlusion. Resting flow was not impaired by this procedure. The measurement performed after establishment of critical coronary stenosis will be denoted as "stenosis" throughout this study.

Within 15 min, mean aortic pressure was reduced to 45 mmHg by withdrawal of arterial blood. When MAP first reached 45 mmHg, this pressure value was maintained by

withdrawal of small amounts of blood for 1 h. Subsequently, measurements were performed (the time point termed "shock").

Infusion of either DCLHb (10%, oncotic pressure 42 mmHg; HemAssist, N. V. Baxter, Hyland Division, Lessines, Belgium) or human serum albumin (HSA; 8.0 g/dl; oncotic pressure 43.8 mmHg; Baxter Blood Substitutes, Deerfield, IL) was then started at 2 $ml \cdot kg\ BW^{-1} \cdot min^{-1}$. Animals were randomly assigned to either group with a random number generator (Visual Basic 3.0 Prof., Microsoft, Redmond, WA) before the study. The amount of fluid administered equaled the amount of plasma withdrawn through the arterial hemorrhage. Microsphere injections and hemodynamic measurements were again performed 1 h after completion of therapy (time point 60′ R).

Data analysis. D was calculated by assessing the heterogeneity of regional perfusion (RD; i.e., SD/mean) repeatedly while reducing the resolution of measurement by averaging adjacent tissue samples. Resolution describes the minimal size of the object that can be observed with a certain method. When RMP is measured with radioactive microspheres, resolution can be changed at will by merely decreasing the size of myocardial samples during dissection of ventricles. Within limits, this is only limited by the number of microspheres within one sample. If microsphere counts are too low, increased methodological error results (2, 35). With the physical act of dissection, the resolution of RMP measurement is set; the minimal size of myocardial regions cannot be changed.

Heterogeneity (expressed as RD) of RMP decreases if spatial resolution is decreased, obeying a power law (1, 32). Decreased resolution translates into larger sizes of myocardial samples. Larger samples contain more vessel bifurcations, which are the sources of blood flow distribution heterogeneity. Only one blood flow value is determined for each myocardial sample. Decreased resolution therefore leads to underestimation of perfusion heterogeneity. One correct resolution of measurement cannot be defined. Therefore, comparison of results from different studies is difficult because resolution varies among studies because of technical differences.

By adding blood flow values of myocardial samples that would have been one single sample with lower resolution (fewer samples dissected from one heart), many different measurement resolutions can be simulated.

Recombinations of myocardial samples were performed in the transmural, transversal, and longitudinal direction. Thus multiple values of RD were obtained with the same physical resolution. Determination of the regression line of RD values and masses of myocardial samples contains measurement errors. In this article, this error was measured, first, with the coefficient of determination, *r*, which can be interpreted as the fraction of the variation of RD that can be explained by the variation of myocardial sample mass. Second, for each calculated slope of the regression line, the SE of this parameter was calculated and reported together with *D*. To this end, we developed a computer program in the statistical programming language R (version 0.63.1; it is available free of charge for Windows and Unix operating systems at, e.g., http://www.ci.tuwien.ac.at/R) and validated it by comparing results with results from a validated computer program (21).

Measured, absolute blood flow values were divided by sample weight, and RD was calculated for the original, dissected, resolution. Lower resolution of measurement was simulated by adding absolute blood flow values of two adjacent samples. After the sum of blood flows was divided by the sum of the weights of each sample pair, RD was calculated for this resolution. For recombination of sample pairs, each of three possible directions (transmural, transversal, and longitudinal) was used. For the complete myocardium, additional simulated resolutions were obtained by recombining absolute perfusion values of 3, 4, 6, 8, 9, 12, and 18 samples. For separate calculations of subendocardial and subepicardial myocardium, recombinations by using only 2, 3, 4, 6, 8, and 12 original samples were possible. For all resolutions, RD was calculated after absolute flows were added and divided by the sum of sample weights.

There is more than one possibility to recombine multiple samples. For example, six samples may be recombined by adding perfusion of three transmurally neighboring and two vertically adjacent samples or vice versa. All possibilities of recombinations were used for all resolutions. The natural logarithm of all RD and sample weight values was taken, and a standard least squares linear regression was performed. All individual RD-weight data pairs, including those with identical sample numbers, were used for regression.

Heterogeneity of RMP decreases if RMP is measured on a larger scale. Therefore, it is important to know how many samples are obtained from one heart. This makes comparison of heterogeneity data from different studies very difficult. Fractal analysis allows measurement of heterogeneity of perfusion on any scale without losing comparability of data. If only one RD value is measured, such a comparison is impossible if resolution varies only slightly. Fractal analysis utilizes the linear relationship of ln(RD) and ln(resolution) over a range of resolutions. When fractal heterogeneity is used, at which part of the line the slope (i.e., *D*) is determined is of little importance. Values can be compared even if heterogeneity was measured with high or with low resolution.

For graphical presentation of distribution of RMP, probability density functions (PDF) were approximated by the empirical distribution of RMP. RMP (Fig. 1) and differences of RMP values from different measurements (see Fig. 6), respectively, were grouped into classes of 0.2 $ml \cdot min^{-1} \cdot g^{-1}$ width. The relative frequency (0–1.0) of values falling into one class was used as one pont of the PDF. All points were connected with a line simulating a continuous function.

Statistics. Statistical analyses were performed with the R statistical software (version 0.63.1). Normal distribution of data was tested with the Shapiro-Wilks test. Myocardial blood flow data were not normally distributed. All other parameters, including heterogeneity of RMP, displayed a Gaussian distribution. Analysis of variance on data or on ranked data (not normally distributed parameters) was used to test the presence of global differences. If this indicated a significant effect, paired *t*-tests or Wilcoxon signed-rank tests, as appropriate, were used to compare data from one measurement with data from the subsequent protocol time point. Comparisons between groups and between myocardial regions were made with the unpaired *t*-test or with the Wilcoxon rank-sum test, as appropriate. Normally distributed data are presented as means ± SD; otherwise, the median (25th/75th percentile) is used. Increased alpha error from repeated testing was corrected for by adjusting the alpha error threshold from $P < 0.05$ to $P < 0.05/n$, where n is the number of sequential tests performed. In the manuscript $P < 0.05$ is used for denoting significant differences, because corrected alpha thresholds serve to ensure that *P* values are actually <0.05.

RESULTS

For induction of hemorrhagic shock, 675 ± 97 ml (274 ml/kg BW; DCLHb group) or 811 ± 118 ml (303 ml/kg BW; HSA group) blood were withdrawn within 15–20 min. This led to arterial hypotension according to the

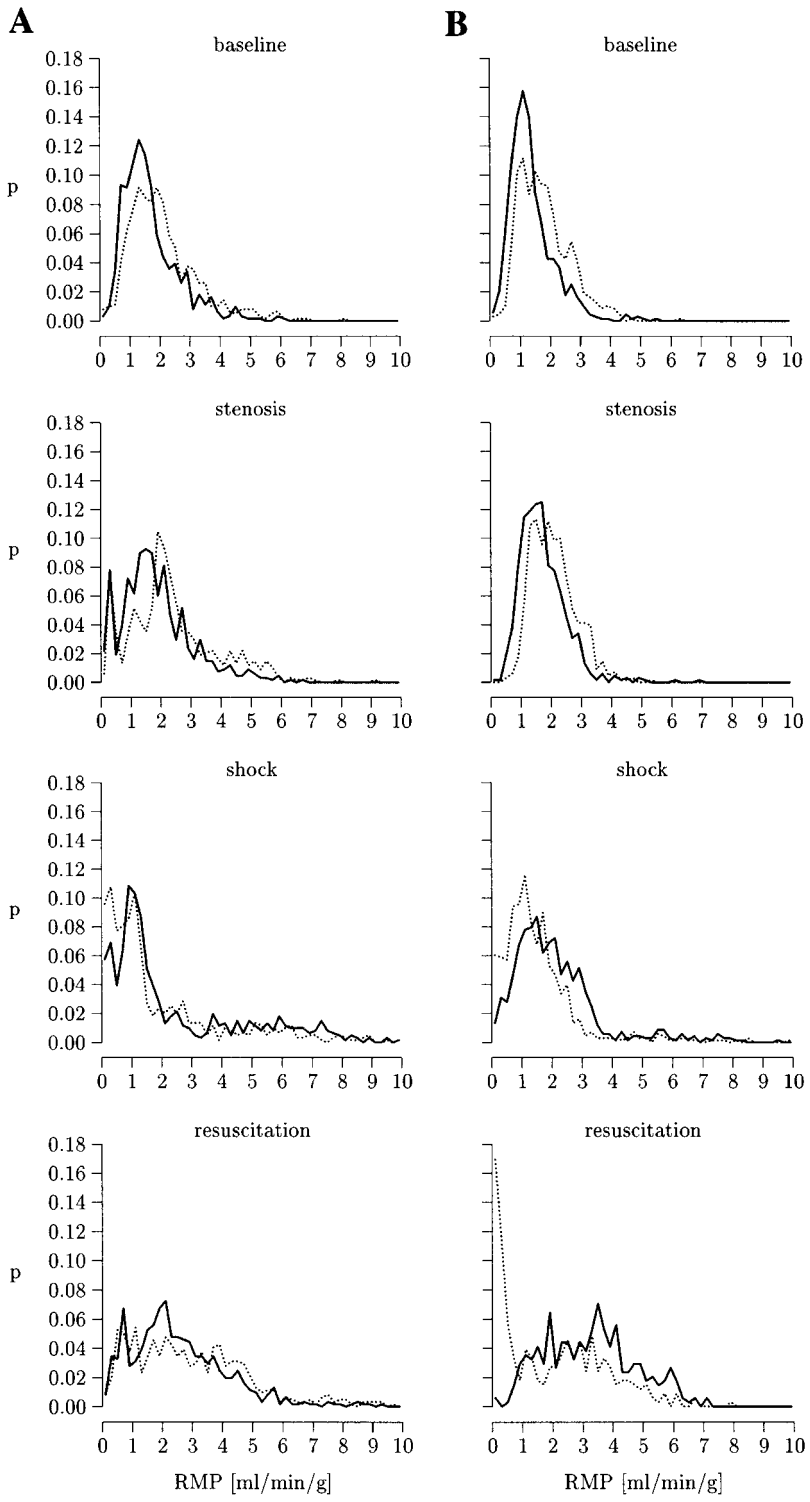

Fig. 1. Probability density functions (PDF) of regional myocardial perfusion (RMP) in diaspirin-cross-linked hemoglobin (DCLHb; *A*) and human serum albumin (HSA; *B*) groups. Dotted lines, subendocardial myocardium; solid lines, subepicardial myocardium; *P*, relative probability of samples to fall into RMP classes of 0.2 $ml \cdot min^{-1} \cdot g^{-1}$ width.

protocol (MAP: DCLHb group, 45 ± 2 mmHg; HSA group, 46 ± 4 mmHg). Within 15–20 min after completion of volume therapy and before the final measurement in the protocol, 5 of 10 HSA-treated animals died from ventricular fibrillation. This was obviously due to arterial hypotension (MAP: HSA group, 69 ± 16 mmHg; DCLHb group, 115 ± 30 mmHg) and LV failure. High LV end-diastolic pressures (LVEDP) indicated reduced LV compliance (LVEDP: 18 ± 9 mmHg in the HSA group vs. 9 ± 4 mmHg in the DCLHb group). At baseline DCLHb- and HSA-treated groups had similar cardiac indexes (DCLHb 4.0 ± 0.8 $l \cdot min^{-1} \cdot m^{-2}$; HSA 4.6 ± 0.5 $l \cdot min^{-1} \cdot m^{-2}$; not significant). Induction of LAD stenosis did not change these values (DCLHb 4.0 ± 0.8 $l \cdot min^{-1} \cdot m^{-2}$; HSA 4.5 ± 0.4 $l \cdot min^{-1} \cdot m^{-2}$; not significant). After 60 min of hemorrhagic shock, there was a severe reduction of CI by 68% (1.3 ± 0.4 $l \cdot min^{-1} \cdot m^{-2}$) in the DCLHb group and 67% in the HSA

Table 1. *Regional myocardial blood flow*

	Baseline	Stenosis	Shock	60′ R
EER				
DCLHb	1.36 ± 0.27	1.38 ± 0.16	0.97 ± 0.30*	1.46 ± 0.47*†
Albumin	1.38 ± 0.30	1.27 ± 0.22	0.78 ± 0.19*	0.63 ± 0.38
MBF_{endo}, $ml \cdot min^{-1} \cdot g^{-1}$				
DCLHb	2.25 (1.35/2.86)	2.40 (2.13/4.39)	1.72 (1.09/4.52)	3.00 (1.93/3.89)
Albumin	2.22 (1.31/2.41)	1.95 (1.81/2.57)	1.56 (1.24/2.09)	3.47 (2.91/3.81)
MBF_{epi}, $ml \cdot min^{-1} \cdot g^{-1}$				
DCLHb	1.68 (1.25/2.22)	1.78 (1.57/3.19)	1.74 (1.13/5.68)	2.45 (1.69/3.22)
Albumin	1.47 (1.15/1.76)	1.75 (1.46/2.16)	1.95 (1.42/2.37)	3.58 (3.12/3.59)
MBF_{norm}, $ml \cdot min^{-1} \cdot g^{-1}$				
DCLHb	1.69 (1.24/2.21)	1.93 (1.68/3.27)*	1.89 (1.17/56.4)‡	2.51 (1.88/3.33)
Albumin	1.58 (0.97/2.02)	1.69 (1.42/2.16)	1.62 (1.17/2.61)	3.86 (3.54/3.89)
MBF_{sten}, $ml \cdot min^{-1} \cdot g^{-1}$				
DCLHb	1.86 (1.19/2.46)	2.05 (1.62/3.12)	1.15 (0.83/4.18)	1.80 (1.59/2.86)
Albumin	1.57 (1.0/1.93)	1.66 (1.49/1.95)	1.09 (0.91/1.84)	2.06 (1.69/2.11)
CPP, mmHg				
DCLHb	88 ± 20	95 ± 19	29 ± 4*	81 ± 31*
Albumin	80 ± 18	80 ± 15	27 ± 3*	26 ± 23†

Values are median (25th percentile/75th percentile) or means ± SD [endocardial-to-epicardial blood flow ratio of stenotic and nonstenoic myocardium (EER) and coronary perfusion pressure (CPP)]. DCLHb, diaspirin-cross-linked hemoglobin group; albumin, albumin group; shock, measurement after 60 min of hemorrhagic shock. 60′ R, measurement 60 min after completion of fluid administration. MBF_{endo}, mean blood flow in subendocardial myocardium; MBF_{epi}, blood flow in subepicardial myocardium; MBF_{norm}, blood flow in normally perfused myocardium; MBF_{sten}, blood flow in poststenotic myocardium. *$P \leq 0.05$ vs. previous time point in the protocol. †$P \leq 0.05$ DCLHb group vs. HSA group. ‡$P \leq 0.05$ poststenotic vs. normal myocardium. (See Ref. 13.)

group ($1.5 \pm 0.4\ l \cdot min^{-1} \cdot m^{-2}$). After infusion of DCLHb the CI was increased ≈2.5-fold to $3.2 \pm 0.7\ l \cdot min^{-1} \cdot m^{-2}$, whereas HSA treatment resulted in a rise of ≈3.7-fold to $5.6 \pm 0.7\ l \cdot min^{-1} \cdot m^{-2}$.

At baseline, endocardial-to-epicardial blood flow ratio (EER) was >1, indicating absence of subendocardial ischemia (Table 1). Induction of critical coronary stenosis did not induce any change of EER (Table 1). After

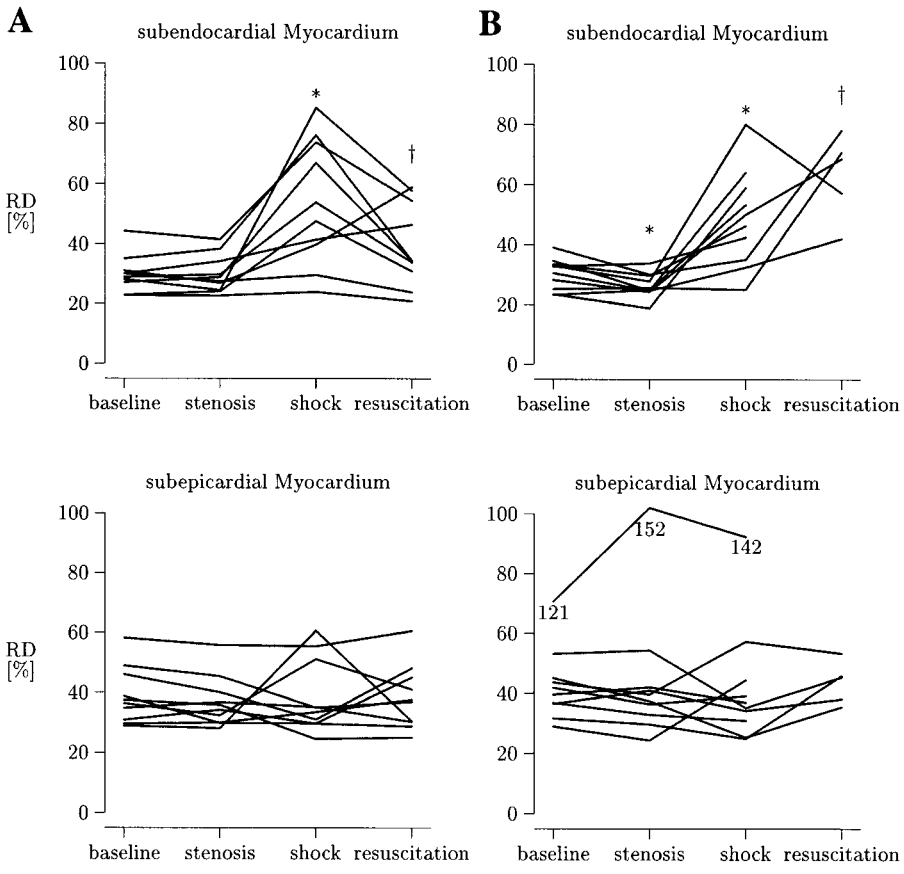

Fig. 2. Relative dispersion (RD; time points in protocol) of RMP at smallest resolution in DCLHb (*A*) and HSA (*B*) groups. *B, bottom*: in the heart of *animal da26*, highly heterogeneous RMP was measured. Ordinates were scaled to yield optimal results for majority of animals. Values of *animal da26* were beyond this scale. For plotting, 50% was subtracted from each value. Subepicardial fractal dimension (*D*) values were also highest in this animal (see Fig. 3). *Significant difference compared with previous time point. †Significant difference between HSA- and DCLHb-treated groups.

Table 2. *Average fractal dimensions, error bars of D, coefficients of determination, and relative dispersions of regional myocardial blood flow*

Group	LV *D*	Error Bar of *D*	Endo *D*	Error Bar of *D*	Epi *D*	Error Bar of *D*
DCLHb						
Baseline	1.27 ± 0.048	0.015 ± 0.004	1.35 ± 0.106	0.032 ± 0.013	1.25 ± 0.057‡	0.019 ± 0.008‡
Stenosis	1.29 ± 0.058	0.016 ± 0.004	1.39 ± 0.104*†	0.028 ± 0.013	1.28 ± 0.056‡	0.023 ± 0.012
Shock	1.26 ± 0.073	0.017 ± 0.012	1.25 ± 0.092*	0.022 ± 0.016	1.31 ± 0.105	0.034 ± 0.018
60′ R	1.25 ± 0.053	0.014 ± 0.006	1.31 ± 0.097	0.026 ± 0.014	1.29 ± 0.104	0.025 ± 0.013
Albumin						
Baseline	1.27 ± 0.085	0.018 ± 0.007	1.31 ± 0.083	0.022 ± 0.005	1.26 ± 0.098	0.020 ± 0.005
Stenosis	1.28 ± 0.104	0.014 ± 0.007	1.27 ± 0.056†	0.018 ± 0.007	1.26 ± 0.116	0.019 ± 0.010
Shock	1.26 ± 0.061	0.018 ± 0.010	1.21 ± 0.093	0.022 ± 0.010	1.32 ± 0.126	0.024 ± 0.016
60′ R	1.22 ± 0.045	0.024 ± 0.016	1.23 ± 0.022	0.023 ± 0.009	1.23 ± 0.047	0.032 ± 0.018
Group	LV r^2	LV RD	Endo r^2	Endo RD	Epi r^2	Epi RD
DCLHb						
Baseline	0.93 ± 0.04	0.37 ± 0.09	0.89 ± 0.06	0.30 ± 0.06	0.93 ± 0.03	0.39 ± 0.09
Stenosis	0.94 ± 0.03	0.36 ± 0.09	0.93 ± 0.05*	0.30 ± 0.06	0.92 ± 0.06	0.37 ± 0.08
Shock	0.90 ± 0.09	0.45 ± 0.15	0.90 ± 0.07	0.54 ± 0.21*	0.86 ± 0.09	0.39 ± 0.12
60′ R	0.92 ± 0.05	0.40 ± 0.11	0.90 ± 0.06	0.40 ± 0.14†	0.90 ± 0.06	0.38 ± 0.11
Albumin						
Baseline	0.88 ± 0.09	0.41 ± 0.13	0.93 ± 0.04	0.30 ± 0.05	0.90 ± 0.08	0.48 ± 0.27
Stenosis	0.92 ± 0.09	0.39 ± 0.22	0.94 ± 0.04	0.26 ± 0.04*	0.90 ± 0.07	0.49 ± 0.37
Shock	0.87 ± 0.12	0.50 ± 0.29	0.85 ± 0.10*	0.49 ± 0.16*	0.90 ± 0.09	0.47 ± 0.35
60′ R	0.78 ± 0.18	0.55 ± 0.10	0.88 ± 0.08	0.63 ± 0.14†	0.81 ± 0.12	0.44 ± 0.07

Values are means ± SD. *D*, fractal dimension; LV, left ventricle; Endo and Epi, subendocardial and subepicardial myocardium, respectively; r^2, coefficient of determination; 60′ R, 60 min after completion of fluid administration; RD, relative dispersion. *$P \leq 0.05$ vs. previous time point in the protocol. †$P \leq 0.05$ DCLHb group vs. HSA group. ‡$P \leq 0.05$ Endo vs. Epi.

hemorrhagic shock for 60 min, EER was significantly reduced to <1 in both groups. In the surviving five animals, after the infusion of HSA there was a nonsignificant reduction of EER. In contrast, application of DCLHb significantly elevated and normalized EER in all animals.

As predicted by the definition of critical stenosis, induction of LAD stenosis did not result in reduction of regional perfusion in the LV subendocardial or subepicardial myocardium (Table 1). During shock, RMP was well preserved in the subepicardial myocardium and only insignificantly reduced in the subendocardial myo-

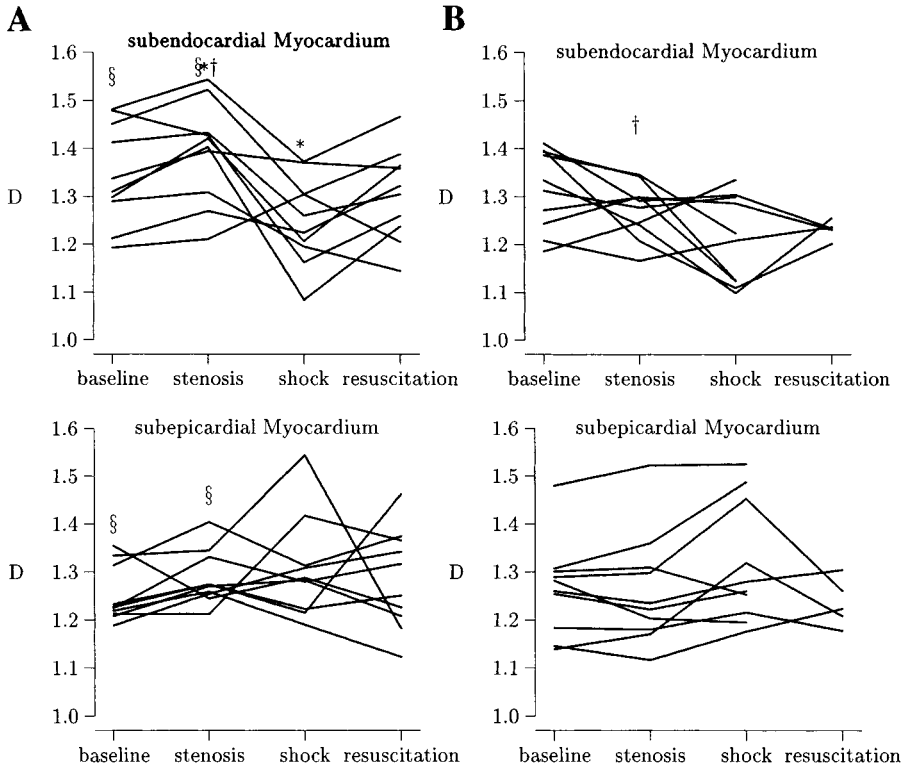

Fig. 3. *D* of RMP measured against time points in protocol (*x*-axis) for DCLHb (*A*) and HSA (*B*) groups. *Significant difference compared with previous time point of protocol, $P < 0.05$. †Significant difference between HSA- and DCLHb-treated groups, $P < 0.05$. §Significant difference between subepicardial and subendocardial *D* of RMP, $P < 0.05$.

Table 3. *Individual fractal dimensions and error bars of D of regional myocardial blood flow*

Animal No.	LV $D \pm$ Error Bar	Endo $D \pm$ Error Bar	Epi $D \pm$ Error Bar
	DCLHb		
da7			
Bl	1.27 ± 0.019	1.41 ± 0.056	1.19 ± 0.016
St	1.31 ± 0.017	1.43 ± 0.044	1.25 ± 0.015
Sh	1.24 ± 0.007	1.26 ± 0.017	1.31 ± 0.015
Re	1.30 ± 0.010	1.30 ± 0.011	1.34 ± 0.014
da11			
Bl	1.20 ± 0.009	1.29 ± 0.035	1.21 ± 0.016
St	1.23 ± 0.008	1.31 ± 0.036	1.27 ± 0.014
Sh	1.19 ± 0.013	1.20 ± 0.019	1.28 ± 0.028
Re	1.19 ± 0.016	1.14 ± 0.018	1.21 ± 0.023
da13			
Bl	1.34 ± 0.013	1.48 ± 0.026	1.22 ± 0.016
St	1.38 ± 0.016	1.43 ± 0.016	1.33 ± 0.030
Sh	1.21 ± 0.015	1.16 ± 0.008	1.28 ± 0.027
Re	1.31 ± 0.011	1.26 ± 0.026	1.32 ± 0.022
da14			
Bl	1.33 ± 0.013	1.30 ± 0.022	1.31 ± 0.019
St	1.40 ± 0.015	1.42 ± 0.017	1.40 ± 0.051
Sh	1.20 ± 0.010	1.21 ± 0.014	1.31 ± 0.033
Re	1.25 ± 0.010	1.36 ± 0.032	1.37 ± 0.028
da22			
Bl	1.24 ± 0.010	1.19 ± 0.019	1.33 ± 0.017
St	1.25 ± 0.012	1.21 ± 0.014	1.34 ± 0.017
Sh	1.39 ± 0.014	1.30 ± 0.034	1.54 ± 0.047
Re	1.18 ± 0.010	1.21 ± 0.021	1.18 ± 0.015
da25			
Bl	1.22 ± 0.021	1.21 ± 0.020	1.22 ± 0.014
St	1.24 ± 0.019	1.27 ± 0.016	1.26 ± 0.013
Sh	1.27 ± 0.014	1.22 ± 0.017	1.19 ± 0.011
Re	1.19 ± 0.012	1.32 ± 0.012	1.12 ± 0.006
da27			
Bl	1.29 ± 0.011	1.45 ± 0.022	1.35 ± 0.039
St	1.27 ± 0.011	1.52 ± 0.017	1.24 ± 0.034
Sh	1.29 ± 0.022	1.31 ± 0.016	1.29 ± 0.052
Re	1.23 ± 0.015	1.39 ± 0.016	1.23 ± 0.032
da29			
Bl	1.22 ± 0.015	1.31 ± 0.030	1.23 ± 0.023
St	1.25 ± 0.018	1.40 ± 0.035	1.27 ± 0.019
Sh	1.16 ± 0.015	1.08 ± 0.010	1.21 ± 0.032
Re	1.31 ± 0.030	1.24 ± 0.025	1.46 ± 0.052
da31			
Bl	1.28 ± 0.019	1.48 ± 0.044	1.21 ± 0.013
St	1.30 ± 0.021	1.54 ± 0.048	1.21 ± 0.011
Sh	1.34 ± 0.048	1.37 ± 0.061	1.42 ± 0.069
Re	1.28 ± 0.015	1.47 ± 0.059	1.37 ± 0.031
da34			
Bl	1.30 ± 0.015	1.34 ± 0.044	1.23 ± 0.017
St	1.30 ± 0.018	1.39 ± 0.040	1.27 ± 0.023
Sh	1.31 ± 0.009	1.37 ± 0.026	1.22 ± 0.025
Re	1.30 ± 0.011	1.37 ± 0.035	1.25 ± 0.027
	Albumin		
da9			
Bl	1.30 ± 0.024	1.40 ± 0.023	1.18 ± 0.027
St	1.33 ± 0.017	1.21 ± 0.019	1.18 ± 0.028
Sh	1.27 ± 0.013	1.11 ± 0.010	1.22 ± 0.030
Re	1.20 ± 0.012	1.20 ± 0.018	1.18 ± 0.029
da12			
Bl	1.22 ± 0.016	1.27 ± 0.022	1.15 ± 0.017
St	1.20 ± 0.013	1.30 ± 0.022	1.12 ± 0.014
Sh	1.24 ± 0.011	1.29 ± 0.033	1.18 ± 0.006
Re	1.20 ± 0.019	1.23 ± 0.021	1.22 ± 0.027
da15			
Bl	1.27 ± 0.016	1.41 ± 0.025	1.14 ± 0.022
St	1.27 ± 0.013	1.29 ± 0.024	1.17 ± 0.019
Sh	1.26 ± 0.006	1.30 ± 0.026	1.32 ± 0.023
Re	1.22 ± 0.011	1.23 ± 0.014	1.21 ± 0.010
da16			
Bl	1.22 ± 0.030	1.24 ± 0.023	1.28 ± 0.023
St	1.22 ± 0.015	1.30 ± 0.008	1.20 ± 0.011
Sh	1.23 ± 0.029	1.12 ± 0.010	1.19 ± 0.009
da17			
Bl	1.22 ± 0.014	1.19 ± 0.016	1.25 ± 0.016
St	1.21 ± 0.005	1.25 ± 0.009	1.22 ± 0.015
Sh	1.24 ± 0.014	1.34 ± 0.029	1.26 ± 0.018
da23			
Bl	1.25 ± 0.025	1.33 ± 0.023	1.29 ± 0.021
St	1.26 ± 0.026	1.24 ± 0.022	1.30 ± 0.024
Sh	1.16 ± 0.019	1.10 ± 0.021	1.45 ± 0.032
Re	1.17 ± 0.032	1.26 ± 0.023	1.26 ± 0.032
da24			
Bl	1.27 ± 0.007	1.31 ± 0.012	1.31 ± 0.023
St	1.27 ± 0.014	1.28 ± 0.010	1.36 ± 0.039
Sh	1.30 ± 0.022	1.30 ± 0.024	1.49 ± 0.050
da26			
Bl	1.47 ± 0.007	1.39 ± 0.029	1.48 ± 0.009
St	1.52 ± 0.002	1.34 ± 0.027	1.52 ± 0.005
Sh	1.40 ± 0.009	1.12 ± 0.009	1.52 ± 0.008
da28			
Bl	1.32 ± 0.019	1.39 ± 0.018	1.30 ± 0.015
St	1.35 ± 0.009	1.35 ± 0.016	1.31 ± 0.015
Sh	1.24 ± 0.020	1.22 ± 0.028	1.25 ± 0.018
da30			
Bl	1.15 ± 0.018	1.21 ± 0.024	1.26 ± 0.022
St	1.15 ± 0.021	1.17 ± 0.019	1.23 ± 0.019
Sh	1.25 ± 0.039	1.21 ± 0.034	1.28 ± 0.050

Bl, St, Sh, and Re: baseline, stenosis, shock, and resuscitation measurements, respectively.

cardium. There was a tendency toward enhanced blood flow secondary to primary resuscitation, but this varied widely within both groups and was insignificant.

In the DCLHb-treated group, there was a significant increase in blood flow in the normally supplied LV wall and a tendency toward enhanced blood flow in the poststenotic area. Irrespective of transmural position (subendocardial, subepicardial), blood flow to the normally perfused myocardium was completely preserved during shock in both groups. In the poststenotic area, there was no significant reduction compared with baseline; however, there was a significantly lower perfusion than in the prestenotic areas in both groups.

Coronary perfusion pressure (CPP) was calculated as diastolic aortic pressure minus LVEDP. There were no differences between groups nor significant alterations of CPP in response to induction of critical coronary stenosis. During shock, CPP was uniformly reduced to approximately one-third of the baseline value. Although HSA infusion (in 5 surviving animals) did not consistently increase CPP, there was almost complete normalization of this parameter on infusion of DCLHb.

PDFs of subendocardial and subepicardial RMP are shown in Fig. 1. Flows >10 $ml \cdot min^{-1} \cdot g^{-1}$ were not plotted to improve graphical appearance of the major-

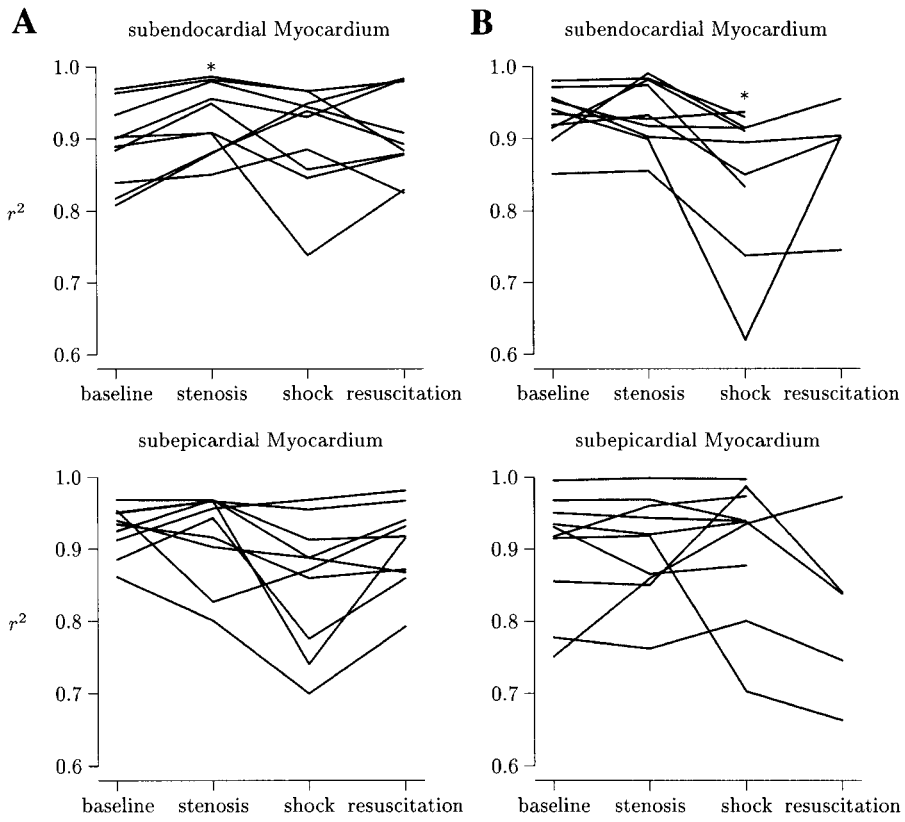

Fig. 4. Coefficients of determination (r) of linear fits of natural logarithms of RD and mass of aggregated myocardial samples for DCLHb (*A*) and HSA (*B*) groups. *x*-Axis, time points in protocol. * Significant difference compared with previous time point of protocol, $P < 0.05$.

ity of RMP values. The slight rightward shift of subendocardial PDFs at baseline and after induction of coronary stenosis is caused by the physiological preferential perfusion of the subendocardial myocardium. During shock, this pattern was reversed; the subendocardial PDF was found slightly left of the subendocardial PDF. In both myocardial layers, a broadening of the distribution occurred; more low-flow and more high-flow regions were present. This broadening was further enhanced after fluid resuscitation. Only in the DCLHb group, the subendocardial PDF was right shifted again in comparison to the subepicardial PDF and resulted in a normalized EER (see Table 1).

RD at the smallest resolution of subendocardial as well as subepicardial perfusion is shown in Fig. 2. Average figures are given in Table 2. There were only changes of the RD in the LV subendocardial myocardium. Induction of coronary stenosis produced a reduction of subendocardial RD in the HSA group. The numerical decrease was small (≈28% of the increase during shock) but consistent and statistically significant. Shock significantly increased subendocardial RD in both groups. Infusion of HSA further increased subendocardial RD in four of five animals; however, this was not statistically tested because of the small number of observations. Administration of DCLHb led to a decrease in RD in 8 of 10 animals. There was a statistical error of $P = 0.036$ to reject the hypothesis "no difference in RD"; however, this was above the corrected threshold of $P = 0.025$. In the subepicardial myocardium of *animal da26*, very high RD of RMP was calculated. Values for subendocardial myocardium were not different from the other animals. No methodological error in RMP measurement was detected. Subepicardial PDF curves of *animal da26* did not display abnormalities except a rightward shift and broadening that were absent in PDFs of subendocardial myocardium.

Subendocardial D as well as subepicardial perfusion are depicted in Fig. 3. Average values of D (together with corresponding error bars) of the complete LV, and subendocardial and subepicardial D are shown in Table 2. D and error bars of D of individual animals are presented in Table 3. At baseline, subendocardial D was significantly higher than subepicardial D in both groups. Induction of critical stenosis increased subendocardial D in the DCLHb group. Although hemorrhagic shock did not affect subepicardial D, there was a significant reduction of subendocardial D in the DCLHb group. The decrease during shock was much greater than the slight but consistent decrease after induction of coronary stenosis in the DCLHb animals.

In the HSA group, there were insignificant reductions of D in 7 of 10 animals in response to critical coronary stenosis ($P = 0.12$) and in 6 of 10 animals during shock ($P = 0.11$). These changes were smaller and less consistent than in the DCLHb animals.

In the DCLHb group, there appeared a tendency toward normalized subendocardial D, but this was not significant. Albumin infusion did not result in large changes in the surviving animals.

As stated in METHODS, the assumption underlying fractal analysis is that the relationship between RD of RMP and resolution of measurement (mass of aggregated samples) is governed by an inverse power law. After the natural logarithms of both parameters are taken, this translates into an inverse linear relation-

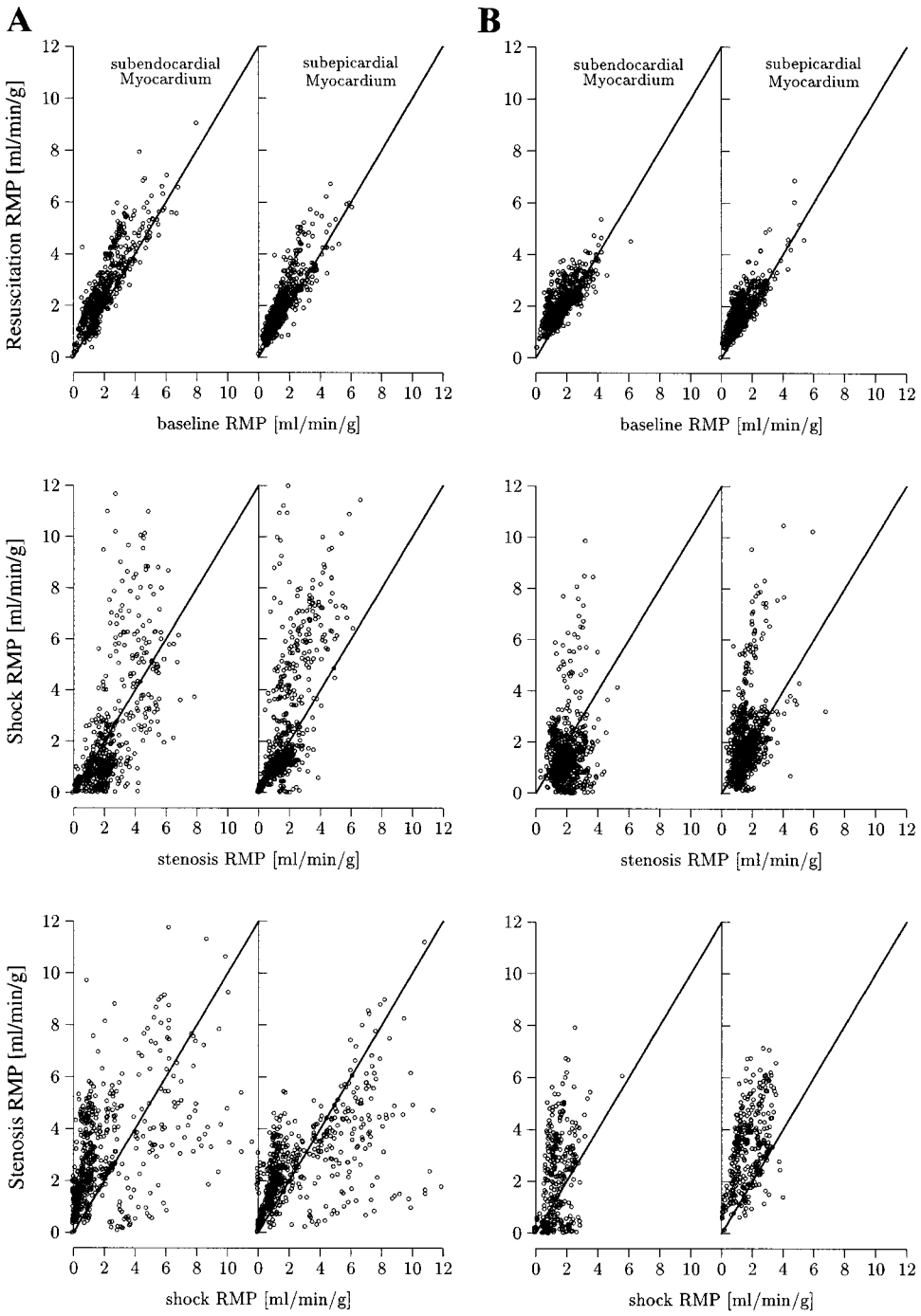

Fig. 5. Changes in perfusion induced by experimental interventions in individual myocardial pieces from DCLHb (*A*) and HSA (*B*) groups. *Left* and *right* halves of each panel denote subendocardial and subepicardial data, respectively; *x*-axis, RMP measured during 1 time point in protocol; *y*-axis, RMP measured during following time point; solid lines, lines of identity. Lack of any change between measurements would result in all data pairs lying on these lines.

ship. Individual *r* values of all linear fits of ln(RD) and ln(mass) are shown in Fig. 4. Average values are given in Table 2.

There was a small increase in *r* after induction of coronary stenosis and no significant change thereafter in the DCLHb group. In contrast, in the HSA group during shock, *r* decreased in seven animals and remained stable in three.

The error bar of the slope of the regression line of ln(RD) and ln(mass) was used to assess the uncertainty of this linear fit. This error was small and did not change in the course of the experiment in any group (see Tables 2 and 3).

Calculation of any heterogeneity parameters implies generalization; no conclusion can be drawn from these parameters as to which changes in perfusion were induced by any intervention in one individual myocardial region. This latter information is presented in Figs. 5 and 6. In Fig. 5, RMP measured at each time point in the protocol is plotted against RMP of the identical myocardial region calculated at the following measurement. Thus if no changes occurred, all data pairs were on a line of identity. In Fig. 6, the distributions of differences of RMP between two measurements are depicted as PDF curves.

Induction of critical coronary stenosis led to a marginal increase of subendocardial as well as subepicar-

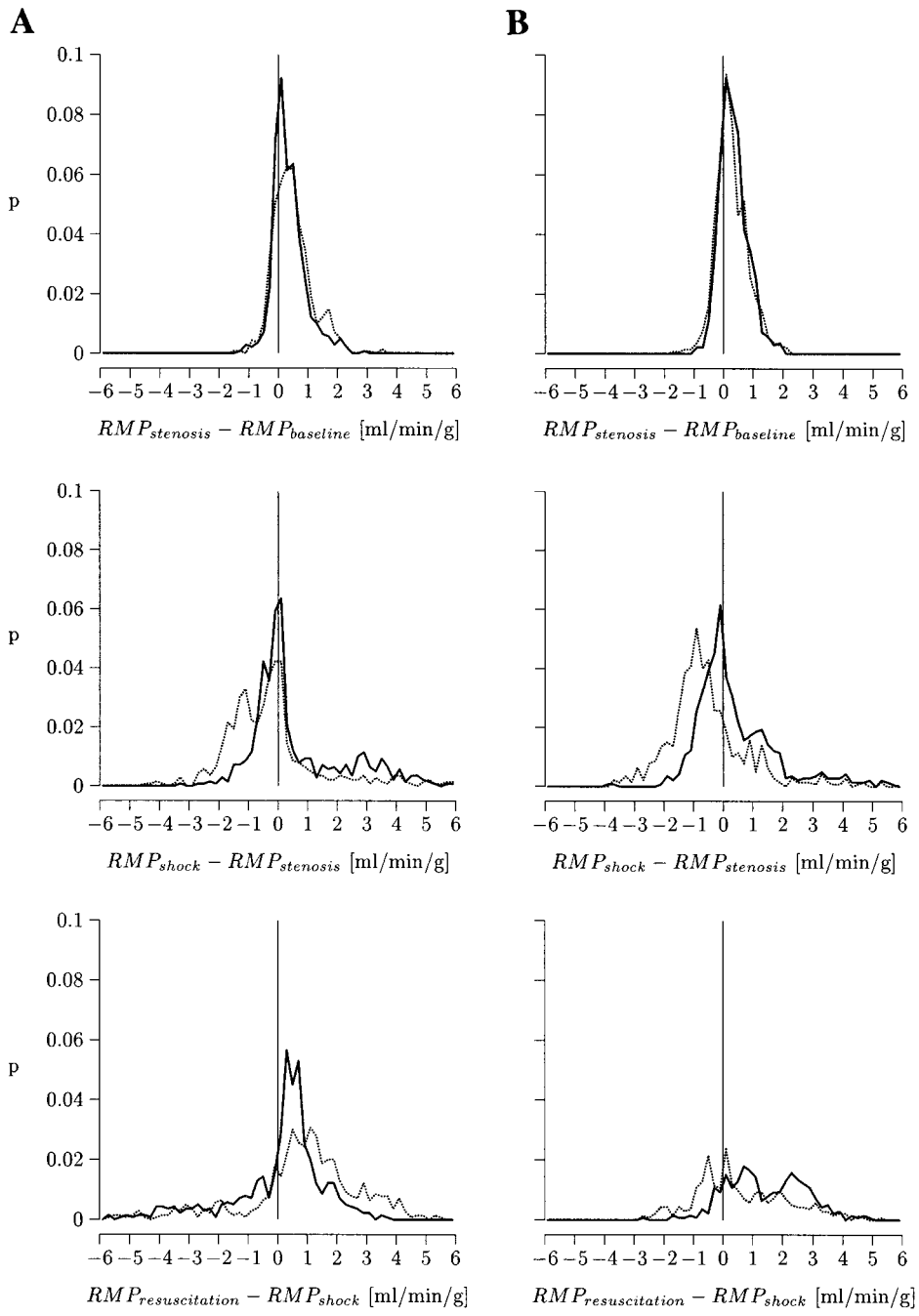

Fig. 6. PDFs of changes in perfusion induced by experimental interventions in individual myocardial pieces from DCLHb (*A*) and HSA (*B*) groups. Dotted lines, PDFs of subendocardial flow differences; solid lines, PDFs of subepicardial flow differences; solid vertical lines, lines through 0 to ease evaluation of PDFs; *P*, relative probability of differences of perfusion during 2 measurements to fall into RMP classes of width 0.2 $ml \cdot min^{-1} \cdot g^{-1}$; *x*-axis, difference in regional myocardial perfusion.

dial RMP in both groups. This is represented by right-shifted PDFs (Fig. 6) and a clustering of data points above the line of identity (Fig. 5). Generally, all high-flow regions remained such during coronary stenosis and vice versa.

The differences in blood flow during shock and blood flow during stenosis alone were predominantly negative in subendocardial myocardium in both groups. However, there were many large increases in flow to individual pieces and more, albeit less extreme, decreases in individual perfusion values.

Resuscitation with DCLHb increased subendocardial perfusion more than subepicardial perfusion. There were many large decreases as well as increases in RMP; however, a large proportion of regions with small RMP was converted to high-flow regions by DCLHb.

In contrast to DCLHb, resuscitation with HSA increased subepicardial perfusion more than subendocardial perfusion. There were less extreme changes than in the DCLHb group. Many low-to-moderate flow regions were transformed to extremely low flow regions in subendocardial myocardium. This latter phenomenon was not present in subepicardial myocardium, where flow almost exclusively increased.

DISCUSSION

The main result of this study was that the fractal model fitted the empirical distributions of RMP during stenosis, shock, and resuscitation. There were, however, decreases in the goodness of fit for the subendocar-

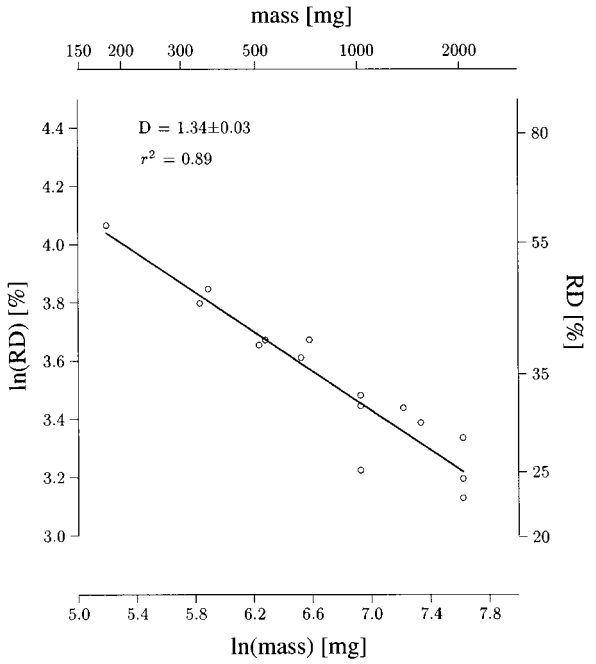

Fig. 7. Typical example of relationship of RD of RMP and aggregated mass of myocardial samples. Data are from *animal da22* at baseline. *Left y*-axis, natural logarithm of RD of RMP [ln(RD); %]; *right y*-axis, RD of RMP (RD; %); *top x*-axis, aggregated mass of myocardial samples (mass; mg); *bottom x*-axis, natural logarithm of aggregated mass of myocardial samples [ln(mass); mg]. Data points having equal or approximately equal mass are derived from different possibilities to recombine larger samples (for further explanation, see *Data analysis*).

dial myocardium during shock in the HSA group. Hemorrhagic shock induced increases in RD of subendocardial perfusion, but the relationship of resolution of measurement and RD became less steep, which translates into a reduced *D*. In subepicardial myocardium, shock did not elicit this effect. Resuscitation with DCLHb induced tendencies toward normalized subendocardial RD and *D* but did not systematically alter subepicardial parameters. Only five animals survived until measurement 60′ R . Therefore, the effects of HSA on RD and *D* could not reliably be evaluated. DCLHb infusion led to a normalized EER in all animals, whereas the surviving HSA-treated animals suffered from a persistently reversed EER.

We have previously shown that hemorrhagic shock reduces *D* of RMP (22). However, in the cited study resuscitation with normal or hypertonic saline, respectively, did not induce normalization of *D*. We performed this study to verify or falsify the hypothesis that more effective fluid resuscitation from hemorrhagic shock would reverse shock-induced reduction of *D* of regional myocardial blood flow.

In our previous study we used either 80% of shed blood volume (SBV) of isotonic saline or one-eighth of this amount of a solution of hypertonic saline and hyperoncotic dextran (small-volume resuscitation) (22). In the present study we attempted to improve resuscitation by using a stable solution of DCLHb. This solution is a hyperoncotic (oncotic pressure 42 mmHg) oxygen carrier and acts as a vasoconstrictor because of nitric oxide scavenging, increased sensitivity of adrenergic receptors, and upregulation of the endothelin system (8, 12). Nitric oxide scavenging has recently been challenged as the sole mechanism of hemoglobin-induced vasoconstriction (29).

DCLHb is a favorable solution for primary resuscitation of hemorrhagic shock, as previous studies in animals have shown. Mortality from hemorrhagic shock in rats can be reduced by DCLHb to the same degree as is achieved by autologous whole blood (4). Gulati and Sen (12) reported that resuscitation from shock with DCLHb produced preferential redistribution of blood flow to the heart and the brain. In the report from these authors, it was also shown that a dose of 50% of SBV resulted in satisfactory resuscitation, which could not be improved by increasing the dose to 100% of SBV. The latter result was the rationale for determining the dose of DCLHb in the present study, namely, the volume of plasma removed with the SBV. Hematocrit is always below 40% in juvenile pigs; this regime led to a DCLHb dose of ~70% of SBV.

Normalization of blood volume after hypovolemic shock dilutes red blood cells and thus reduces arterial oxygen content. Because hemoglobin in a cellular solution can transport oxygen (14, 16, 30), the dilutional effect of fluid therapy of shock can be offset by DCLHb. As a control solution, 8.0% HSA was used. This solution has the same oncotic pressure as DCLHb and, as a protein, has similar pharmacokinetic properties, at least over the limited posttreatment observation period in this study.

At baseline, subepicardial myocardium *D* values were in the range of what has been reported previously for baboons, sheep, and rabbits (1). Subendocardial *D*, however, was higher than reported before for whole ventricles and significantly above subepicardial values. We also calculated *D* for complete ventricles and found values in the range that was previously reported. Differences in *D* from subendocardial myocardium and subepicardial myocardium between our results and those from previous studies were absent after induction of hemorrhagic shock.

D values of the whole ventricle were lower in this study than in our previous paper (22). In contrast to the latter, in the present article subepicardial *D* values were in the range of LV *D* values, and subendocardial *D* values were higher than both LV and subepicardial *D*. Despite these, in part extreme, differences, the effects of hemorrhagic shock were similar in both studies. Hemorrhagic shock reduced subendocardial *D* more than subepicardial *D*. However, in contrast to our previous study LV *D* values were not altered by shock. The most prominent difference between both studies is that hypertonic and normal saline further changed LV *D* in the same direction as did shock, whereas DCLHb but not HSA evoked a tendency toward an increase in subendocardial *D*.

The differences in *D* cannot be explained by differences in calculations. We used identical numbers of RD-mass data pairs for linear regression, and similar algorithms (implemented in different programming languages) were applied. All radioactive microsphere injections and measurements were performed by the

same person in both studies. Despite major differences in different parameters, the main result of fractal analysis in both studies, reduction of subendocardial *D* during shock, was identical in both reports.

There was no significant difference of RD values at maximum resolution between left ventricular subepicardial and subendocardial myocardium. However, before shock, average epicardial RD values were higher than subendocardial values, but this was not statistically significant. In our previous study, RD of RMP was lower than the values in this paper. This reflects the higher resolution of RMP measurement in the present study (≈10% lower sample weight). Subendocardial RD was lower than subepicardial RD in both studies. Whereas in this paper subepicardial RD was not altered during shock, in the saline study there was an increase in subepicardial RD. This increase was much smaller than subendocardial changes, paralleling the tendency observed in this study.

It is no contradiction that higher RD at maximum resolution and significantly lower subendocardial myocardium *D* occurred. RD at one resolution represents only one point on the linear log-log plot of heterogeneity and resolution, whereas *D* represents a measure of the slope of this line (see Fig. 7). The line may rotate around one point, leaving RD values of one resolution unchanged, whereas others are increased or decreased. Because of different techniques of perfusion measurement and different resolution, comparison of RD from the present study with data from previous reports of other research groups is difficult. However, taking into account the dependence of RD on sample mass, there appears to be no difference between baseline RD values in the present study compared with previous reports (1, 18, 25).

It is striking that, in either experimental group, *D* values derived from subepicardial myocardium did not change in response to shock, whereas subendocardial *D* values were significantly or tendentially reduced after induction of hemorrhagic shock. RD of the RMP of subendocardial and subendocardial myocardium, respectively, confirmed these findings. There was no alteration of subepicardial RD in shock, but subendocardial RD was significantly increased in subendocardial myocardium in both groups.

These results confirm our previous findings (22) that shock in the presence of critical coronary stenosis most strongly affects subendocardial perfusion heterogeneity. Subendocardial edema and consecutive compression of intramyocardial vessels (3), as well as preferential swelling of myocytes in the subendocardial myocardium (17), might be mechanisms causing this difference.

In conclusion, we have confirmed that hemorrhagic shock in the presence of coronary stenosis reduces subendocardial RMP *D*. Blood flow to subendocardial myocardium is more susceptible to changes in flow distribution, whereas subepicardial perfusion is relatively unaffected.

Despite the insignificant change in *D* values of subendocardial RMP ($P = 0.066$) and RD ($P = 0.036$), it cannot be ignored that there was a strong tendency toward normalization after infusion of DCLHb.

We therefore conclude that our hypothesis can cautiously be considered verified: rapid and effective fluid therapy with DCLHb did induce a tendency toward restoration of normal distribution of regional myocardial blood flow. In previous experiments (22), we have investigated the effects of resuscitation from shock with isotonic and hypertonic saline solutions on RMP distribution. None of these fluids has proven efficacious in this respect. It remains to be investigated whether resuscitation with autologous or homologous blood is able to restore heterogeneity of RMP after hemorrhagic shock.

The authors gratefully acknowledge Alke Schropp's valuable contribution to experimentation and data acquisition as well as the professional care for the animals by Otto Frisch and team.

Address for reprint requests and otherv correspondence: M. Kleen, Institute for Surgical Research, Univ. of Munich, Marchioninistr. 15, 81366 Munich, Germany (E-mail: kleen@icf.med.uni-muenchen.de).

Received 12 January 1999; accepted in final form 22 September 1999.

REFERENCES

1. **Bassingthwaighte, J. B., R. B. King, and S. A. Roger.** Fractal nature of regional myocardial blood flow heterogeneity. *Circ. Res.* 65: 578–590, 1989.
2. **Buckberg, G. D., J. C. Luck, D. B. Payne, J. I. E. Hoffman, J. P. Archie, and D. E. Fixler.** Some sources of error in measuring regional blood flow with radioactive microspheres. *J. Appl. Physiol.* 31: 598–604, 1971.
3. **Carlson, E. L., S. L. Selinger, J. Utley, and J. I. Hoffman.** Intramyocardial distribution of blood flow in hemorrhagic shock in anesthetized dogs. *Am. J. Physiol.* 230: 41–49, 1976.
4. **Chang, T., and R. Varma.** Effect of a single replacement of one of ringer lactate, hypertonic saline/dextran, 7 g% albumin, stroma-free hemoglobin, O-raffinose polyhemoglobin or whole blood on the long term survival of unanesthetized rats with lethal hemorrhagic shock after 67% acute blood loss. *Biomater. Artif. Cells Immobilization Biotechnol.* 20: 503–510, 1992.
5. **Chilian, W. M.** Coronary microcirculation in health and disease. Summary of an NHLBI workshop. *Circulation* 95: 522–528, 1997.
6. **Cousineau, D. F., C. A. Goresky, J. R. Rouleau, and C. P. Rose.** Microsphere and dilution measurements of flow and interstitial space in dog heart. *J. Appl. Physiol.* 77: 113–120, 1994.
7. **Deussen, A.** Local myocardial glucose uptake is proportional to, but not dependent on blood flow. *Pflügers Arch.* 433: 488–496, 1997.
8. **Freas, W., R. Llave, M. Jing, J. Hart, P. McQuillan, and S. Muldoon.** Contractile effects of diaspirin cross-linked hemoglobin (DCLHb) on isolated porcine blood vessels. *J. Lab. Clin. Med.* 125: 762–767, 1995.
9. **Gewirtz, H., H. A. Skopicki, S. A. Abraham, H. Castano, R. E. Dinsmore, N. M. Alpert, and A. J. Fischman.** Quantitative PET measurements of regional myocardial blood flow: observations in humans with ischemic heart disease. *Cardiology* 88: 62–70, 1997.
10. **Gould, K. L., K. Lipscomb, and G. W. Hamilton.** Physiologic basis for assessing critical coronary stenosis. Instantaneous flow response and regional distribution during coronary hyperemia as measures of coronary flow reserve. *Am. J. Cardiol.* 33: 87–94, 1974.
11. **Gross, W., R. Schosser, and K. Messmer.** MIC-III—an integrated software package to support experiments using the radioactive microsphere technique. *Comput. Programs Biomed.* 33: 65–85, 1990.
12. **Gulati, A., and A. Sen.** Dose-dependent effect of diaspirin cross-linked hemoglobin on regional blood circulation of severely hemorrhaged rats. *Shock* 9: 65–73, 1998.

13. **Habler, O., M. Kleen, A. Pape, F. Meisner, G. Kemming, and K. Messmer.** Diaspirin crosslinked hemoglobin (DCLHb) reduces mortality of severe hemorrhagic shock in pigs with critical coronary stenosis. *Crit. Care Med*. In press.
14. **Habler, O., and K. Messmer.** Hemoglobin solutions: effects on tissue oxygenation. Tissue oxygenation in acute medicine. In: *Update on Intensive Care Emergency Medicine*. Berlin: Springer, 1998, vol. 33, p. 291–306.
15. **Heymann, M. A., B. D. Payne, J. I. Hoffman, and A. M. Rudolph.** Blood flow measurements with radionuclide-labeled particles. *Prog. Cardiovasc. Dis*. 20: 55–79, 1977.
16. **Horn, E., T. Standl, S. Wilhelm, E. Jacobs, U. Freitag, M. Freitag, and J. Schulte am Esch.** Bovine hemoglobin increases skeletal muscle oxygenation during 95% artificial arterial stenosis. *Surgery* 121: 411–418, 1997.
17. **Horton, J., and D. Poehlmann.** Regional coronary blood flow in canine hemorrhagic shock. *Circ. Shock* 23: 271–283, 1987.
18. **Iversen, P. O., and G. Nicolaysen.** Fractals describe blood flow heterogeneity within skeletal muscle and within myocardium. *Am. J. Physiol. Heart Circ. Physiol*. 268: H112–H116, 1995.
19. **Kassab, G. S., C. A. Rider, N. J. Tang, and Y. C. Fung.** Morphometry of pig coronary arterial trees. *Am. J. Physiol. Heart Circ. Physiol*. 265: H350–H365, 1993.
20. **Kleen, M., O. Habler, and K. Messmer.** A tool for balancing activity from isotopes used for the radioactive microsphere method. *Comp. Meth. Prog. Biomed*. 53: 81–86, 1997.
21. **Kleen, M., O. Habler, B. Zwissler, and K. Messmer.** Programs for assessment of spatial heterogeneity of regional organ blood flow. *Comp. Meth. Prog. Biomed*. 55: 51–57, 1998.
22. **Kleen, M., M. Welte, M., P. Lackermeier, O. Habler, G. Kemming, and K. Messmer.** Myocardial blood flow heterogeneity in shock and small-volume resuscitation in pigs with coronary stenosis. *J. Appl. Physiol*. 83: 1832–1841, 1997.
23. **Mangano, D., M. Hollenberg, G. Fegert, L. Meyer, M. London, J. Tubau, and W. Krupski.** Perioperative myocardial ischemia in patients undergoing noncardiac surgery. I. Incidence and severity during the 4 day perioperative period. *J. Am. Coll. Cardiol*. 17: 843–850, 1991.
24. **Mangano, D., G. Wong, M. London, J. Tubau, and J. Rapp.** Perioperative myocardial ischemia in patients undergoing noncardiac surgery. II. Incidence and severity during the 1st week after surgery. *J. Am. Coll. Cardiol*. 17: 851–857, 1991.
25. **Maningas, P. A.** Resuscitation with 7.5% NaCl in 6% dextran-70 during hemorrhagic shock in swine: effects on organ blood flow. *Crit. Care Med*. 15: 1121–1126, 1987.
26. **Matsumoto, T., M. Goto, H. Tachibana, Y. Ogasawara, K. Tsujioka, and F. Kajiya.** Microheterogeneity of myocardial blood flow in rabbit hearts during normoxic and hypoxic states. *Am. J. Physiol. Heart Circ. Physiol*. 270: H435–H441, 1996.
27. **Mori, H., M. Chujo, S. Haruyama, H. Sakamoto, Y. Shinozaki, M. Uddin-Mohammed, A. Iida, and H. Nakazawa.** Local continuity of myocardial blood flow studied by monochromatic synchrotron radiation-excited X-ray fluorescence spectrometry. *Circ. Res*. 76: 1088–1100, 1995.
28. **Pickelmann, S., D. Nolte, R. Leiderer, E. Schuetze, and K. Messmer.** Attenuation of postischemic reperfusion injury in striated skin muscle by diaspirin-cross-linked Hb. *Am. J. Physiol. Heart Circ. Physiol*. 275: H361–H368, 1998.
29. **Rohlfs, R., E. Bruner, A. Chiu, A. Gonzales, M. Gonzales, D. Magde, M. J. Magde, K. Vandegriff, and R. Winslow.** Arterial blood pressure responses to cell-free hemoglobin solutions and the reaction with nitric oxide. *J. Biol. Chem*. 273: 12128–12134, 1998.
30. **Standl, T. G., W. Reeker, G. Redmann, E. Kochs, C. Werner, and J. Schulte am Esch.** Haemodynamic changes and skeletal muscle oxygen tension during complete blood exchange with ultrapurified polymerized bovine haemoglobin. *Int. Care Med*. 23: 865–872, 1997.
31. **VanBavel, E., and J. Spaan.** Branching patterns in the porcine coronary arterial tree. Estimation of flow heterogeneity. *Circ. Res*. 71: 1200–1212, 1992.
32. **Van Beek, J. H., S. A. Roger, and J. B. Bassingthwaighte.** Regional myocardial flow heterogeneity explained with fractal networks. *Am. J. Physiol. Heart Circ. Physiol*. 257: H1670–H1680, 1989.
33. **Visser, K., J. Meeder, J. Van Beek, E. Van der Wall, A. Willemsen, and P. Blanskma.** A mathematical model for the heterogeneity of myocardial perfusion using nitrogen-13-ammonia. *J. Nucl. Med*. 39: 1312–1319, 1998.
34. **Welte, M., P. Lackermeier, O. Habler, M. Kleen, G. Kemming, L. Frey, B. Zwissler, and K. Messmer.** Effect of hypertonic saline/dextran on poststenotic myocardial perfusion, metabolism, and function during resuscitation from hemorrhagic shock in anesthetized pigs. *Shock* 7: 119–130, 1997.
35. **Zwissler, B., R. Schosser, V. Iber, M. Weiss, C. Schwickert, P. Spengler, and K. Messmer.** Methodological error, and spatial variability of organ blood flow measurements using radiolabeled microspheres. *Res. Exp. Med*. 191: 47–63, 1991.